Journal of Engineering Mathematics **44:** 297–309, 2002.

Water-wave scattering by two symmetric circular-arc-shaped thin plates

B.N. MANDAL* and RUPANWITA GAYEN (NÉE CHOWDHURY)
Physics and Applied Mathematics Unit, Indian Statistical Institute, 203, B.T. Road, Calcutta - 700 108, India;
*(*Corresponding author, e-mail : biren@isical.ac.in)*

Received 23 January 2002; accepted in revised form 13 July 2002

Abstract. The problem of surface water-wave scattering by two symmetric circular-arc-shaped thin plates submerged in deep water is investigated in this paper assuming linear theory. The problem is formulated in terms of hypersingular integral equations which are solved approximately using finite series involving Chebyshev polynomials of the second kind. The coefficients of the finite series are obtained numerically by a collocation method. Very accurate numerical estimates for the reflection and the transmission coefficients are then obtained. The numerical results are depicted graphically against the wave number for different arc lengths of the plates, the depth of their submergence and the separation length. Known results for a circular cylinder and horizontal straight plate are recovered.

Key words: circular-arc-shaped plates, hypersingular integral equation, reflection coefficient, water-wave scattering.

1. Introduction

Within the framework of linearised theory of water waves, scattering of surface water waves by obstacles of various geometrical shapes constitutes an extremely important class of problems which have been investigated by many researchers for many decades by using various mathematical and computational techniques. The importance of this class of problems lies in their possible engineering application in designing models of breakwaters which are constructed to protect coastal areas from the hazards of the rough sea. Only very few problems in this class involving scattering of normally incident surface water waves by fixed vertical thin plates in deep water can be solved explicitly. For example, Ursell [1] obtained an explicit solution when the obstacle has the form of a partially immersed thin vertical plate or a submerged thin vertical barrier extending infinitely downwards. He used an integral-equation formulation based on Havelock's expansion of the water-wave potential. Evans [2] obtained an explicit solution, when the obstacle is in the form of a submerged thin vertical plate, by using the complex-variable technique leading to solving a Riemann-Hilbert boundary-value problem. Porter [3] obtained an explicit solution for an obstacle in the form of a thin vertical wall with a gap, by using an integral-equation formulation based on an appropriate use of Green's integral theorem. Many other researchers studied vertical-barrier problems using various mathematical techniques. A detailed account of these can be found in Mandal and Chakrabarti [4, Chapter 4]. Also, Levine and Rodemich [5] investigated water wave scattering by *two* thin vertical plates which intersect the free surface and are immersed up to the same depth in deep water, for explicit solution. They used complex-variable theory to obtain the reflection and transmission coefficients in terms of integrals whose integrands are complicated functions of elliptic

integrals. The complementary problem of two thin vertical barriers submerged from the same depth below the free surface and extending infinitely downwards was also solved explicitly by Jarvis [6] using complex variables.

For obstacles in the form of thin curved plates submerged in deep water, it is no longer possible to obtain an explicit solution for water-wave scattering problems. However, it may then be possible to use some approximate methods to obtain numerical estimates for the quantities of physical interest, namely the reflection and transmission coefficients. For example, Parsons and Martin [7] considered water-wave scattering by a single thin curved plate submerged in deep water, whose parametric equations are given, and formulated the problem in terms of a hypersingular integral equation for the discontinuity of the potential function describing the motion in the fluid, across the curved plate. They presented numerical results for the reflection coefficient for a submerged circular arc which is convex upwards and symmetric about the vertical through the centre of the circle whose arc assumes the position of the plate. Shortly afterwards, McIver and Urka [8] used two different techniques, one involving the method of matched series expansions and the other involving a variational approximation procedure, to obtain numerical results for the reflection coefficient for a curved plate shaped like the top of a circle submerged in deep water. Their objective was to compare the reflective properties of a circular-arc-shaped plate with those for a submerged full circle for assessing the suitability of using circular plates in the construction of a water-wave lens which would focus waves prior to extracting energy from them.

A pair of symmetric circular-arc-shaped thin plates submerged in deep water may serve as a simple model for breakwaters, since these are easy to construct and simple to implement from an engineering point of view. As such, the mathematical study of water-wave scattering by such a pair of obstacles, particularly their reflective properties, is not without significance. Unlike scattering problems involving two symmetric thin vertical barriers, either partially immersed in deep water up to the same depth [5] or fully submerged in deep water from the same depth below the free surface and extending infinitely downwards [6], which admit explicit solutions, the scattering problem involving two symmetric circular-arc-shaped thin plates submerged in deep water cannot be solved explicitly. However, the reflective properties of such a pair of obstacles can be studied numerically by using an approximate method based on a hypersingular-integral-equation formulation of the problem in a manner somewhat similar to that used by Parsons and Martin [7] for studying wave scattering by a single submerged circular-arc-shaped thin plate. Thus, the present paper is concerned with a generalisation of the water-wave-scattering problem involving a single arc-shaped thin plate to two symmetric circular-arc-shaped thin plates submerged in deep water. The line joining the centres of the circles, whose arcs assume the positions of the two plates, is horizontal, and the two arcs are symmetrically placed with respect to the vertical through the mid point of this line. Exploiting the geometrical symmetry, the scattering problem is split into two separate problems involving symmetric and anti-symmetric potential functions describing the resulting motion in the fluid due to an incoming surface water-wave train incident on the plates. Appropriate use of Green's integral theorem, followed by utilization of the boundary condition on the plates, produces two integro-differential equations, which are interpreted as equivalent to two hypersingular integral equations in the discontinuities of the symmetric and anti-symmetric potential functions across one of the two plates. These hypersingular integral equations are solved numerically by approximating discontinuities of the potential functions across the plate in terms of two finite series involving Chebyshev polynomials of the second kind followed by a collocation

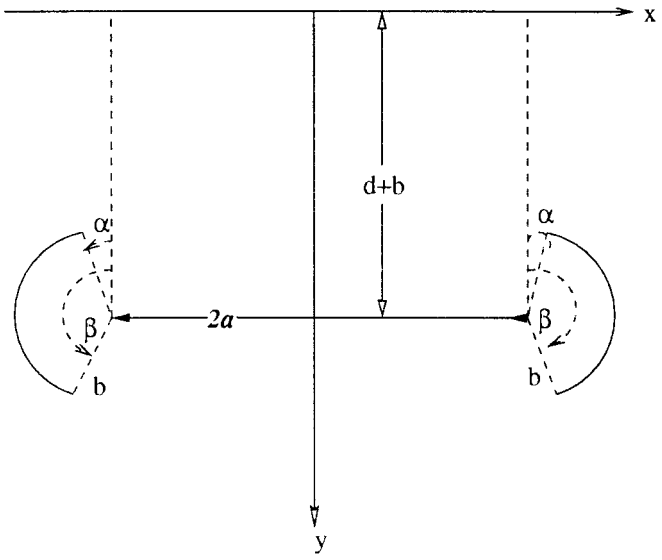

Figure 1. Geometrical sketch of the problem.

method. The reflection and transmission coefficients are then computed numerically by using these solutions.

Numerical results for the reflection coefficients showing variation of the depth of submergence of the plates, arc lengths of the plates and separation length between the centres of the circles whose arcs assume the positions of the plates, are depicted graphically against the wave number in a range of figures. For the case of semicircular plates with vertical diameters, the reflection coefficient is seen to become very small when the separation between the centres, *i.e.*, the distance between the vertical diameters of the semicircular plates, is made very small. However, in this case, the two semicircles almost assume the form of a full circle, and the phenomenon of very small reflection is consistent with the classical result obtained long ago by Dean [9] and Ursell [10], namely that a horizontal circular cylinder submerged in deep water experiences no reflection by a normally incident incoming train of surface water waves. Again, numerical results are obtained for a submerged obstacle in the form of a convex lens whose two sides consist of intersecting circular arcs of the same radius and are symmetric about the vertical mid section. For some frequencies the phenomena of total reflection and total transmission are observed to occur for such an obstacle. Somewhat similar phenomena are also seen to occur when the effect of transition from a circular-arc-shaped plate that is symmetric about the vertical, to a horizontal plate of the same arc length on the reflection coefficient, is considered.

2. Formulation of the problem

A Cartesian co-ordinate system is chosen in which the y-axis is taken vertically downwards into the fluid region and the plane $y = 0$ is the rest position of the free surface. Let two symmetric circular-arc-shaped thin plates $\Gamma_i (i = 1, 2)$ be submerged in deep water and occupy the positions described by arcs of two circles of the same radius b with centres at $(\pm a, d + b)$, as illustrated in Figure 1.

A point (x, y) on the plate $\Gamma_i (i = 1, 2)$ can be expressed as

$$x = \pm(a + b\sin\theta),\ \ y = d + b(1 - \cos\theta), \alpha \leq \theta \leq \beta, \tag{2.1}$$

where α, β are the angles made by the radii through the upper and lower ends of the plates with the vertical, and further, a, b and the angles α, β must satisfy the inequality

$$a \geq \max(-b\sin\alpha, -b\sin\beta). \tag{2.2}$$

Assuming linear theory, incompressible and inviscid fluid, and irrotational motion, we may describe an incoming surface wave train by the potential function $\mathfrak{Re}\left\{\phi^{\text{inc}}(x, y)\mathrm{e}^{-\mathrm{i}\sigma t'}\right\}$ where t' is the time, σ is the frequency and

$$\phi^{inc}(x, y) = 2\mathrm{e}^{-Ky - \mathrm{i}K(x-a)} \tag{2.3}$$

with $K = \sigma^2/g$, g being the acceleration due to gravity. Let this incoming wave train be incident on the two arc-shaped plates from the direction of $x = \infty$. Let the resulting motion in the fluid be described by the potential function $\mathfrak{Re}\left\{\phi(x, y)\mathrm{e}^{-\mathrm{i}\sigma t'}\right\}$; then $\phi(x, y)$ satisfies

$$\nabla^2\phi = 0 \text{ in the fluid region}, \tag{2.4}$$

where ∇^2 is the two-dimensional Laplacian operator,

$$K\phi + \phi_y = 0 \text{ on} y = 0, \tag{2.5}$$

$$\phi_n = 0 \text{ on } \Gamma_i (i = 1, 2), \tag{2.6}$$

where ϕ_n denotes the normal derivative at a point on $\Gamma_i (i = 1, 2)$,

$$r^{1/2}\nabla\phi \text{ is bounded as } r \to 0, \tag{2.7}$$

where r is the distance from any submerged edge of Γ_i,

$$\nabla\phi \to 0 \text{ as } y \to \infty, \tag{2.8}$$

and

$$\phi(x, y) \to \begin{cases} \phi^{\text{inc}}(x, y) + R\phi^{\text{inc}}(-x, y) & \text{as } x \to \infty, \\ T\phi^{\text{inc}}(x, y) & \text{as } x \to -\infty \end{cases} \tag{2.9}$$

where R and T denote, respectively, the reflection and transmission coefficients (complex); their numerical estimation is the principal aim here.

3. Method of solution

Because of the geometrical symmetry of the two plates about the y-axis, $\phi(x, y)$ can be split into its symmetric and antisymmetric parts $\phi^s(x, y)$ and $\phi^a(x, y)$ so that

$$\phi(x, y) = \phi^s(x, y) + \phi^a(x, y), \tag{3.1}$$

where

$$\phi^s(-x, y) = \phi^s(x, y), \phi^a(-x, y) = -\phi^a(x, y). \tag{3.2}$$

Thus, we can restrict our analysis to the region $x \geq 0$ only. Now the functions $\phi^{s,a}(x, y)$ satisfy (2.4) to (2.8) together with

$$\phi_x^s(0, y) = 0, \phi^a(0, y) = 0, y > 0. \tag{3.3}$$

Let the behaviour of $\phi^{s,a}(x, y)$ for large x be represented by

$$\phi^{s,a}(x, y) \to \mathrm{e}^{-Ky} \left\{\mathrm{e}^{-\mathrm{i}K(x-a)} + R^{s,a}\mathrm{e}^{\mathrm{i}K(x-a)}\right\} \text{as} x \to \infty, \tag{3.4}$$

where $R^{s,a}$ are unknown constants, and because of (2.9), are related to R and T by

$$R, T = \frac{1}{2}\left(R^s \pm R^a\right)\mathrm{e}^{-2\mathrm{i}Ka}. \tag{3.5}$$

For obtaining representations of $\phi^{s,a}(x, y)$ satisfying (2.4), (2.5), (2.8) and (2.9) we require the source potential function $G(x, y; \xi, \eta)$ due to a line source at $(\xi, \eta)(\eta > 0)$ as given by [11]

$$G(x, y; \xi, \eta) = \log\frac{r}{r'} - 2\int_C \frac{\mathrm{e}^{-k(y+\eta)}}{k - K}\cos k(x - \xi)\mathrm{d}k \tag{3.6}$$

with $r, r' = \left\{(x - \xi)^2 + (y \mp \eta)^2\right\}^{1/2}$ and the path C is along the positive real axis in the complex k-plane indented below the pole at $k = K$.

We now apply Green's integral theorem to the functions $\phi^{s,a} - \mathrm{e}^{-Ky-\mathrm{i}K(x-a)}$ and $\mathcal{G}^{s,a}(x, y; \xi, \eta)$ where

$$\mathcal{G}^{s,a}(x, y; \xi, \eta) = G(x, y; \xi, \eta) \pm G(-x, y; \xi, \eta), \tag{3.7}$$

in the region bounded by the lines $y = 0, 0 \le x \le X; x = X, 0 \le y \le Y; y = Y, 0 \le x \le X; x = 0, 0 \le y \le Y$; a small circle of radius ϵ with centre at (ξ, η) and a contour enclosing the arc Γ_1, and ultimately we make $X, Y \to \infty, \epsilon \to 0$ and shrink the contour enclosing Γ_1 into the two sides of Γ_1, to obtain

$$\phi^{s,a}(\xi, \eta) = 2\mathrm{e}^{-K\eta+\mathrm{i}Ka}(\cos K\xi, -\mathrm{i}\sin K\xi) - \frac{1}{2\pi}\int_{\Gamma_1} F^{s,a}(p)\mathcal{G}_{n_p}^{s,a}(x, y; \xi, \eta)\mathrm{d}s_p, \tag{3.8}$$

where $p \equiv (x, y)$ is a point on Γ_1, $F^{s,a}(p)$ are the discontinuities of $\phi^{s,a}(x, y)$ across Γ_1 at p, and $\mathcal{G}_{n_p}^{s,a}$ denote the normal derivative to $\mathcal{G}^{s,a}$ at the point $p \in \Gamma_1$. It should be noted that the unknown functions $F^{s,a}(p)$ vanish at the end points of Γ_1 while their derivatives have square-root singularities at the end points.

Use of the boundary condition (2.6) rewritten as

$$\phi_{n_q}^{s,a} = 0 \text{ on } \Gamma_1,$$

where $q \equiv (\xi, \eta)$ is a point on Γ_1, produces the integro-differential equations

$$\frac{\partial}{\partial n_q}\int_{\Gamma_1} F^{s,a}(p)\mathcal{G}_{n_p}^{s,a}(p; q)\mathrm{d}s_p = 2\pi\frac{\partial}{\partial n_q}\left[2\mathrm{e}^{-K\eta+\mathrm{i}Ka}\,(\cos K\xi, -\mathrm{i}\sin K\xi)\right], q \in \Gamma_1. \tag{3.9}$$

The order of differentiation and integration in (3.9) can be interchanged, provided the integrals are interpreted as Hadamard finite-part integrals [5]. This leads to the hypersingular integral equations

$$\text{⨍}\!\!\!\!\!\!-_{\Gamma_1} F^{s,a}(p)\mathcal{G}_{n_p n_q}^{s,a}(p; q)\mathrm{d}s_p = 4\pi\left[\mathrm{e}^{-K\eta+\mathrm{i}K\xi}\,(\cos K\xi, -\mathrm{i}\sin K\xi)\right]_{n_q}, q \in \Gamma_1 \tag{3.10}$$

where the cross on the integral sign indicates that the integrals are to be interpreted as Hadamard finite-part integrals.

Let $\mathbf{n}_p$ and $\mathbf{n}_q$ denote the unit normals at the points p and q, respectively, on Γ_1, then

$$\mathbf{n}_p = (\sin\theta_t, -\cos\theta_t),\ \mathbf{n}_q = (\sin\theta_\tau, -\cos\theta_\tau), \tag{3.11}$$

where

$$\theta_{t,\tau} = \frac{\alpha+\beta}{2} + \frac{\beta-\alpha}{2}(t,\tau), -1 < t, \tau < 1, \tag{3.12}$$

the co-ordinates of the points $p \equiv (x, y)$ and $q \equiv (\xi, \eta)$ on Γ_1 being parametrically expressed as

$$\begin{aligned} x &= a + b\sin\theta_t,\ y = \mathrm{d} + b(1-\cos\theta_t), -1 \le t \le 1, \\ \xi &= a + b\sin\theta_\tau,\ \eta = \mathrm{d} + b(1-\cos\theta_\tau), -1 \le \tau \le 1. \end{aligned} \tag{3.13}$$

The hypersingular integral equations (3.10) are now rewritten as

$$\text{⨍}\!\!\!\!\!\!-_{-1}^{1} f^{s,a}(t)\left[-\frac{1}{(\tau-t)^2} + \mathcal{K}^{s,a}(\tau,t)\right]\mathrm{d}t = h^{s,a}(\tau),\ -1 < \tau < 1, \tag{3.14}$$

where we have used the notations $f^{s,a}(t)$ for $F^{s,a}(p)$, and

$$\begin{aligned} \mathcal{K}^{s,a}(\tau,t) \;=\; & -\frac{\Theta^2}{4}\left[\frac{1}{\sin^2\frac{\Theta}{2}(\tau-t)} - \frac{4}{\Theta^2(\tau-t)^2}\right] \\ & + b^2\Theta^2\left[-\cos(\theta_\tau-\theta_t)\left\{\frac{Y^2-X^2}{(X^2+Y^2)^2} + \frac{2KY}{X^2+Y^2} + 2K^2\Phi_0(X,Y)\right\}\right. \\ & -2\sin(\theta_\tau-\theta_t)\left\{\frac{XY}{(X^2+Y^2)^2} + \frac{KX}{X^2+Y^2} + K^2\Psi_0(X,Y)\right\} \\ & \pm\cos(\theta_\tau-\theta_t)\frac{Z^2-X_1^2}{(X_1^2+Z^2)^2} \pm \sin(\theta_\tau-\theta_t)\frac{2X_1Z}{(X_1^2+Z^2)^2} \\ & \mp\cos(\theta_\tau+\theta_t)\left\{\frac{Y^2-X_1^2}{(X_1^2+Y^2)^2} + \frac{2KY}{X_1^2+Y^2} + 2K^2\Phi_0(X_1,Y)\right\} \\ & \left.\pm 2\sin(\theta_\tau+\theta_t)\left\{\frac{X_1Y}{(X_1^2+Y^2)^2} + \frac{KX_1}{X_1^2+Y^2} + K^2\Psi_0(X,Y)\right\}\right] \end{aligned} \tag{3.16}$$

with

$$\begin{aligned} &\Theta = \frac{1}{2}(\beta-\alpha),\ X = b(\sin\theta_t - \sin\theta_\tau),\ X_1 = 2a + b(\sin\theta_t + \sin\theta_\tau), \\ &Y = 2(d+b) - b(\cos\theta_t + \cos\theta_\tau),\ Z = b(\cos\theta_\tau - \cos\theta_t), \\ &\Phi_0(X,Y),\ \Psi_0(X,Y) = \int_C \frac{\mathrm{e}^{-kY}}{k-K}(\cos kX, \sin kX)\mathrm{d}k, \end{aligned} \tag{3.17}$$

and

$$h^{s,a}(\tau) = 4\pi K b\Theta \mathrm{e}^{-K\eta + \mathrm{i}Ka}\left(\cos(K\xi+\theta_\tau),\ -\mathrm{i}\sin(K\xi+\theta_\tau)\right). \tag{3.18}$$

We have to solve the hypersingular integral equations (3.14), keeping in mind that $f^{s,a}(\pm 1) = 0$.

As in Parsons and Martin [7] the integrals in (3.17) can be expanded as

$$\int_C \frac{\mathrm{e}^{-kY}}{k-K}\begin{pmatrix}\cos\\ \sin\end{pmatrix} kX\,\mathrm{d}k = -\mathrm{e}^{-KY}\left\{(\log Kr_1 - \mathrm{i}\pi + \gamma)\begin{pmatrix}\cos\\ \sin\end{pmatrix} KX\right)$$
$$+\theta_1\begin{pmatrix}\sin\\ -\cos\end{pmatrix} KX\Bigg)\Bigg\} + \sum_{m=1}^{\infty}\frac{(-Kr_1)^m}{m!}\left(\frac{1}{1}+\frac{1}{2}+\ldots+\frac{1}{m}\right)\begin{pmatrix}\cos\\ -\sin\end{pmatrix} m\theta_1\Bigg) \tag{3.19}$$

where $r_1^2 = X^2 + Y^2$, $\theta_1 = \tan^{-1}(X/Y)$ and $\gamma = 0{\cdot}5772\ldots$ is Euler's constant.

We now approximate $f^{s,a}(t)$ as

$$f^{s,a}(t) = (1-t^2)^{1/2}\sum_{n=0}^{N} a_n^{s,a} U_n(t), \tag{3.20}$$

where $U_n(t)$ is the Chebyshev polynomial of the second kind and $a_n^{s,a}(n = 0, 1, \ldots, N)$ are unknown constants to be found. The square-root factor in (3.20) ensures that $f^{s,a}(t)$, *i.e.*, $F^{s,a}(p)$, have the correct behaviour at the end points. Using the expansions (3.20) in (3.14) we obtain

$$\sum_{n=0}^{N} a_n^{s,a} A_n^{s,a}(\tau) = h^{s,a}(\tau),\ -1 < \tau < 1 \tag{3.21}$$

where

$$A_n^{s,a}(\tau) = \pi(n+1)U_n(\tau) + \int_{-1}^{1}(1-t^2)^{1/2}\mathcal{K}^{s,a}(\tau,t)U_n(t)\mathrm{d}t. \tag{3.22}$$

To find the unknown constants $a_n^{s,a}(n = 0, 1, \ldots, N)$, we put $\tau = \tau_j(j = 0, 1, \ldots, N)$ in (3.22) to obtain the linear systems

$$\sum_{n=0}^{N} a_n^{s,a} A_n^{s,a}(\tau_j) = h^{s,a}(\tau_j),\ j = 0, 1, \ldots, N \tag{3.23}$$

where τ_j's are collocation points and are chosen as [7]

$$\tau_j = \cos\frac{2j+1}{2N+2}\pi,\ j = 0, 1, \ldots, N. \tag{3.24}$$

The two linear systems (3.23) can be solved numerically by any standard method to determine $a_n^{s,a}(n = 0, 1, \ldots, N)$ numerically. Here we have used the Gauss-Jordan method.

To find the reflection and transmission coefficients $|R|$ and $|T|$ we first obtain the quantities $R^{s,a}$ by making $\xi \to \infty$ in the representations (3.8) for $\phi^{s,a}(\xi, \eta)$ and comparing with (3.4), with (x, y) replaced by (ξ, η). For this we require the asymptotic results

$$\mathcal{G}^{s,a}(x, y; \xi, \eta) \to -4\pi\,\mathrm{e}^{-K(y+\eta)+\mathrm{i}K\xi}(\mathrm{i}\cos kx, \sin kx) \text{ as } \xi \to \infty. \tag{3.25}$$

Thus we find that

$$
\begin{aligned}
R^{s,a} &= \pm e^{2iKa} + 2e^{iKa} \int_{\Gamma_1} F^{s,a}(p) \frac{\partial}{\partial n_p} \left[e^{-k\eta y} (i \cos kx, \sin kx) \right] ds_p \\
&= \pm e^{2iKa} + 2Kb\Theta e^{iKa} \sum_{n=0}^{N} a_n^{s,a} \int_{-1}^{1} (1-t^2)^{1/2} U_n(t) \\
&\quad e^{-K(d+b(1-\cos\theta_t))} \begin{pmatrix} i\cos \\ \sin \end{pmatrix} (Ka + Kb \sin\theta_t + \theta_t) \Big) dt.
\end{aligned} \tag{3.26}
$$

The integrals in (3.26) can be evaluated numerically by standard methods. Thus, once $a_n^{s,a} (n = 0, 1 \ldots, N)$ are found numerically by solving the linear systems (3.23), $R^{s,a}$ can be computed numerically from (3.26) for different values of the parameters $Kb, d/b, a/b$ and Θ. Having found $R^{s,a}$, we can obtain the reflection and transmission coefficients R and T numerically by using (3.5). Also, as $|R|$ and $|T|$ must satisfy the identity

$$|R|^2 + |T|^2 = 1. \tag{3.27}$$

We can use this as a partial check on the correctness of the numerical results obtained for $R^{s,a}$ by using (3.26).

4. Numerical results

The reflection coefficient $|R|$ is computed numerically for various values of the different parameters. In Table 1 we display the numerical results for $|R|$ showing its convergence with the truncation size N of the finite series (3.20) for different arc lengths of the two plates by choosing $d/b = 0{\cdot}5, a/b = 1{\cdot}0,\ Kb = 1{\cdot}5$ and $\alpha = 0$, $\beta = \pi/2$ and π. It is observed from the table that the truncation size depends on $\beta - \alpha$, *i.e.*, the arc lengths of the plates when d/b and a/b are kept fixed. However, if we keep the arc length fixed and vary the separation parameter a/b, keeping d/b fixed, or vary the depth parameter, keeping a/b fixed, then, for a fixed wave number, the corresponding tabular values of $|R|$ (not shown here) would produce different truncation sizes for the convergence. Thus, the truncation size depends on all the different parameters associated with the geometrical position of the plates, as well as the wave number Kb. In our numerical computations for every data appropriate safeguard has been taken on the truncation size, so as to produce numerical results that are correct up to almost five decimal places.

In Table 2, a representative set of values $|R|, |T|$ and $|R|^2 + |T|^2$ against Kb for $d/b = 0{\cdot}1, a/b = 1{\cdot}5, \alpha = 0, \beta = \pi$ are given. It is observed that $|R|^2 + |T|^2$ almost coincides with unity for different Kb. Thus, the reflection and transmission coefficients $|R|$ and $|T|$ computed by using the formulae (3.5), where $R^{s,a}$ are computed by using the relations in (3.26), satisfy the energy equality $|R|^2 + |T|^2 = 1$. This may provide a partial check on the correctness of the numerical results obtained here, although this cannot be regarded as a sufficient requirement for the correctness of the numerical results. However, some other checks are also provided later in which the results obtained by following the present numerical procedure for the limiting cases of a submerged full circle and a submerged horizontal plate, produce known numerical results existing in the literature obtained by following some other methods.

Figure 2 depicts $|R|$ against Kb for two semi-circular arc-shaped plates with vertical diameters ($\alpha = 0, \beta = \pi$) and constant depth parameter $d/b = 0{\cdot}5$ for different separation lengths. The main feature of the curves for $|R|$ is the occurrence of zeros of $|R|$ as a function of the

Table 1. Reflection coefficient $|R|$ ($d/b = 0{\cdot}5$, $a/b = 1{\cdot}0$, $Kb = 1{\cdot}5$, $\alpha = 0$)

N	$\beta = \pi/2$	$\beta = \pi$
0	0·17198	0·72171
2	0·30619	0·15170
4	0·29101	0·28328
6	0·29089	0·27598
8	0·29089	0·27534
10		0·27541
12		0·27541

Table 2. $|R|$ and $|T|$ ($d/b = 0{\cdot}1$, $a/b = 1{\cdot}5$, $\alpha = 0$, $\beta = \pi$)

Kb	$\lvert R\rvert$	$\lvert T\rvert$	$\lvert R\rvert^2 + \lvert T\rvert^2$
0·5	0·567566	0·823327	1·000000
1·0	0·783176	0·621799	1·000000
1·5	0·462642	0·886545	1·000000

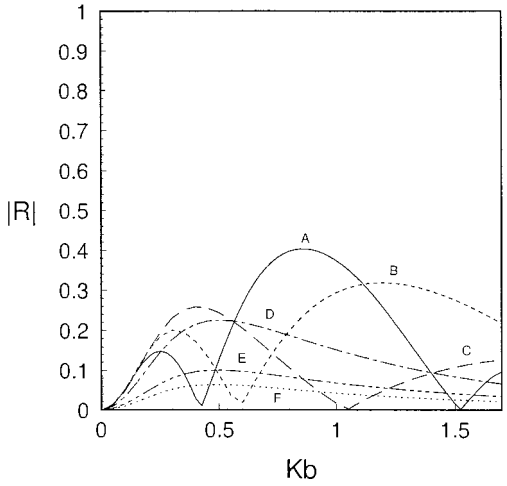

Figure 2. Reflection coefficient for two half-circles ($\alpha = 0$, $\beta = \pi$) d/b = 0·5, a/b = 1·5(A), 1·0(B) 0·5(C) 0·1(D) 0·001(E) 0·00001(F)

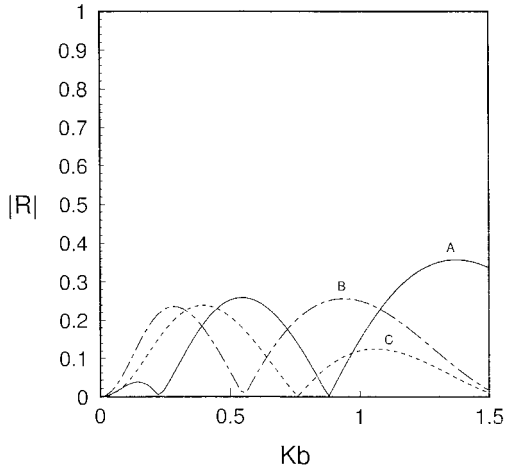

Figure 3. Reflection coefficient for different arc-lengths a/b=1·5, d/b=0·5, $\alpha = 70$, $\beta = 340$(A), 280(B), 220(C)

wave number. As the separation length a/b decreases, the zeros of $|R|$ are shifted towards the right. Another important feature is the overall decrease of $|R|$ with the decrease of a/b. When the separation length becomes negligibly small ($a/b = 0{\cdot}0001$), then $|R|$ also becomes very small for all wave numbers. This result is consistent with the classical result that $|R|$ is identically zero for a full circular arc, *i.e.*, for a circular cylinder submerged in deep water irrespective of the depth and the frequency of the incident wave field, obtained first by Dean [9] and established rigorously by Ursell [10] soon afterwards, since the two semi-circular arc-shaped plates with vertical diameters assume almost the shape of a full circle when a/b becomes very small. This result also provides another partial check on the correctness of the numerical results obtained here.

Figure 3 depicts $|R|$ against Kb for fixed depth ($d/b = 0{\cdot}5$) and separation length ($a/b = 1{\cdot}5$) but different arc lengths of the plates ($\alpha = 70°$; $\beta = 340°, 280°, 220°$). It shows the effect of different arc lengths on $|R|$ for fixed depth and separation length. Here also the occurrence

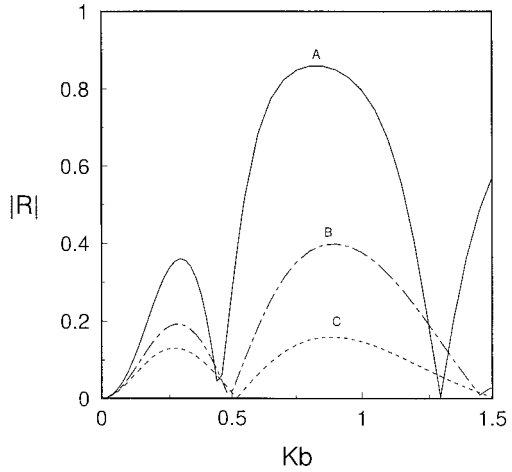

Figure 4. Reflection coefficient for different depths. a/b=1·5, $\alpha = 5$, $\beta = 150$, 0·1(A), 0·5(B), 1·0(C)

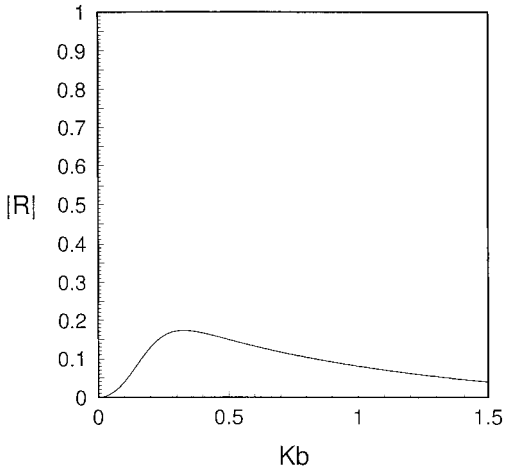

Figure 5. Reflection coefficient for two almost full circles. $\alpha = 0$, $\beta = 359$; $\alpha = -90$, $\beta = 269$, a/b=1·5, d/b=0·5

of zeros of $|R|$ as a function of the wave number is the principal feature. As the arc length decreases the zeros of $|R|$ are shifted towards the right. Also, the overall reflection coefficient decreases with a decrease of the arc length. This is quite plausible, since in general less energy is reflected by the plates when the arc length decreases, due to the incident wave train facing less resistance.

Figure 4 displays the dependence of $|R|$ for a fixed pair of circular arc-shaped plates ($\alpha = 5°, \beta = 150°$) on the depth parameter ($d/b = 0{\cdot}1, 0{\cdot}5, 1{\cdot}0$). It is observed from this figure that the overall reflection coefficient decreases with the increase of the depth, and the shifting of zeros of $|R|$ with the increase of d/b is of not much significance. The overall decrease of $|R|$ with the increase of d/b is expected, since the disturbance created by the incident wave train does not penetrate much below the free surface and, as such, less energy is reflected by an obstacle whose depth below the free surface is considerable.

The reflection coefficient for two submerged almost full circles (two circular cylinders) is shown in Figure 5. For $a/b = 0{\cdot}5, d/b = 1{\cdot}5$, $|R|$ for almost two full circles is obtained by choosing $\alpha = 0°, \beta = 359°$ and also by choosing $\alpha = -90°$ and $\beta = 269°$, and the two curves for $|R|$ for these two sets of values of α and β almost coincide. We have also checked that for other sets of values of α, β which produce almost full circles, the corresponding curves for $|R|$ practically coincide. This can be regarded as another partial check on the correctness of the numerical method utilized here. Again, this figure demonstrates that, although a single submerged cylinder experiences no reflection, submerged twin cylinders do experience reflection for an incoming surface wave train.

The result for a submerged lens-shaped body whose two sides consist of intersecting circular arcs of the same radius and symmetric about the vertical mid section of the lens, can be obtained by suitable choices of α, β and a/b. One such choice is $\alpha = -\frac{\pi}{6}, \beta = \pi + \frac{\pi}{6}$ and $a/b = \sin\frac{\pi}{6} = 0{\cdot}5$. Figure 6 displays $|R|$ for such a lens-shaped obstacle for different values of the depth parameter d/b ($d/b = 0{\cdot}5, 0{\cdot}1, 0{\cdot}05, 0{\cdot}01, 0{\cdot}0$). For moderate values of the depth parameter ($d/b = 0{\cdot}5, 0{\cdot}1$) $|R|$, regarded as a function of the wave number Kb, first

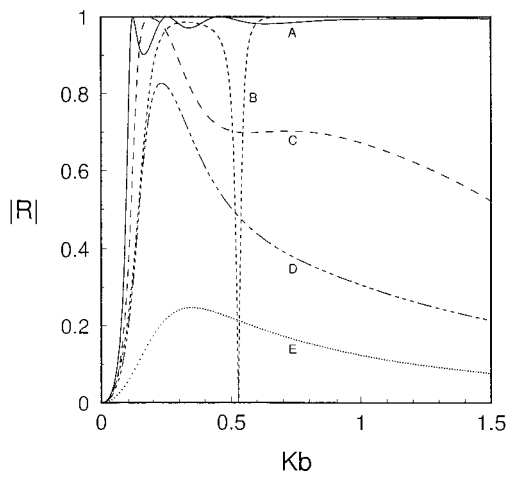

Figure 6. Reflection Coefficient for lens shaped obstacle. $\alpha = -\pi/6$, $\beta = 7\pi/6$, a/b=0·5, d/b = 0 (A), 0·01(B), 0·05(C), 0·1(D), 0·5(E)

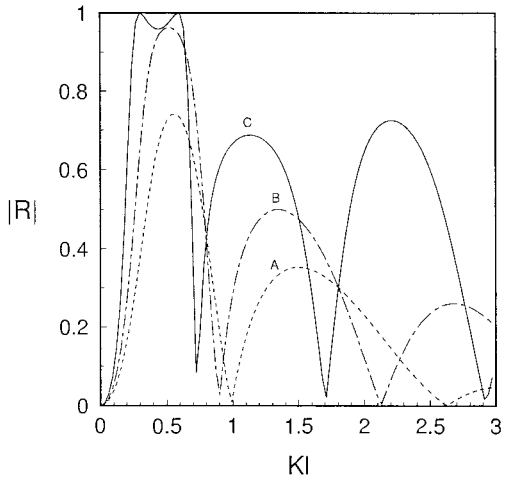

Figure 7. Reflection coefficient for small $\beta - \alpha$, d/l=0·1, a/l=0·0, $\alpha = 0$, $= \pi/5$(A), $\pi/10$(B), $\pi/180$(C)

increases as Kb increases from 0, attains a maximum value and then decreases as Kb further increases. However, for a small value of d/b ($d/b = 0{\cdot}05$), $|R|$ sharply increases from zero value to almost unity and then decreases as Kb further increases. As d/b is further decreased ($d/b = 0{\cdot}01$), $|R|$ sharply increases almost to unity as before, but then again decreases sharply to zero and again almost becomes unity as the wave number further increases. This is perhaps due to interaction of waves between the free surface and the sharp upper edge of the convex lens-shaped body because of its proximity to the free surface. For $d/b = 0$ the upper edge is still below the free surface, but it is nearer to the free surface compared to the previous situations. In this case $|R|$ initially increases sharply from zero to unity, then oscillates near the unit value for moderate values of the wave number and becomes almost unity as the wave number further increases. This type of a lens-shaped body submerged not much below the free surface appears to possess the property of almost total reflection for most values of the wave number, and thus may act as an efficient breakwater. Also, the phenomenon of occurrence of total reflection for some frequencies may have some bearing on the search for trapped modes in the presence of submerged obstacles.

The effect of transition from a circular-arc-shaped plate that is symmetric about the vertical, to a horizontal plate of same arc length, on $|R|$, can be visualised by putting $a/l = 0$, where $2l$ is the fixed arc length of the plate, and by decreasing the difference $\beta - \alpha$ but increasing b such that $b(\beta - \alpha)$ has the constant value l. The Figure 7 displays $|R|$ against the new wave number Kl (when $d/l = 0{\cdot}1$) for $\alpha = 0^\circ$ and the choices $\beta = 36^\circ, 18^\circ$ and 1° when $l = b\beta$ is kept fixed. The configuration $\alpha = 0^o$, $\beta = 1^\circ$ can be regarded as an almost straight horizontal plate. The qualitative features of the curves for $|R|$ due to the transition from a circular-arc-shaped plate to a horizontal plate are observed to be the same as given by Parsons and Martin [7] who, however, investigated water-wave scattering by a single circular-arc-shaped plate. This observation may also be regarded as another partial check on the correctness of the numerical results obtained here.

For various configurations of the two circular-arc-shaped plates (including the situations when they assume the form of an almost full circle or a horizontal plate) submerged in deep water, it is observed that the long-wave limit of the reflection coefficient is zero. This is in conformity with the observation of Martin and Dalrymple [12] and McIver [13] who confirmed, by using the method of matched asymptotic expansions, that the reflection coefficient becomes zero in the long-wave limit.

5. Conclusion

The reflective properties of two symmetric circular-arc-shaped plates submerged in deep water due to a train of incoming surface water waves have been investigated here assuming linear theory. The solution method is based on hypersingular-integral-equation formulation of the problem wherein the hypersingular integral equations are solved numerically and the solutions are utilized to obtain numerical estimates for the reflection coefficient for various configurations of the plates. This method of solution was utilized earlier in the literature to investigate the reflective properties of a single circular-arc-shaped plate submerged in deep water. The particular geometry of two symmetric circular-arc-shaped plates considered here is somewhat general, and the results for a single almost full circle, two full circles, an almost horizontal plate or a convex lens-shaped obstacle, whose two sides consist of intersecting circular arcs of the same radius and are symmetric about the vertical mid section, have been obtained as special cases. In all the cases, the reflection coefficient is depicted against the wave number in a number of figures and the main features of the reflection curves have been observed and their implications discussed. Results have been obtained, some of which might be expected such as a decrease of the reflection coefficient as the plates become more deeply submerged or almost zero reflection as the circular-arc-shaped plates assume the configuration of an almost full circle. The main feature in these curves is the occurrence of zero reflection for some frequencies of the incoming wave train. Also, for the special configuration of the twin plates as they assume the form of an obstacle in the form of a convex lens, total reflection occurs for some wave numbers. This may have some bearing on the search for trapped modes in the presence of submerged obstacles. It is also important to note that, while for a fully submerged circular cylinder, the reflection coefficient vanishes identically for all wave numbers, this is not true for two circular cylinders.

This method of hypersingular integral equations is most general in the sense that it can be adopted to study water-wave-interaction problems involving obstacles in the form of thin curved plates having any geometrical shape. In the present paper we have considered only a pair of symmetric circular-arc-shaped plates, which are submerged in deep water. If the plates are not symmetrically situated, then also this method can be utilized, although its decomposition into two separate problems will no longer be possible. The case when the plates are partially immersed can be tackled by this method, but then at one end point which corresponds to the point (or points) of interaction of the plates with the free surface, a boundedness condition has to be taken care of in solving the hypersingular integral equations numerically.

Acknowledgement

The authors thank the referees for their comments and suggestions to improve the paper towards the present form. This work is supported by National Board for Higher Mathematics, Mumbai.

References

1. F. Ursell, The effect of a fixed vertical barrier on surface waves in deep water. *Proc. Camb. Phil. Soc.* 43 (1947) 374–382.
2. D.V. Evans, Diffraction of surface waves by a submerged vertical plate. *J. Fluid Mech.* 40 (1970) 433–451.
3. D. Porter, The transmission of surface waves through a gap in a vertical barrier. *Proc. Camb. Phil. Soc.* 71 (1972) 411–421.
4. B.N. Mandal and A. Chakrabarti, *Water Wave Scattering by Barriers*. Southampton: WIT Press (2000) 390 pp.
5. H. Levine and E. Rodemich, Scattering of surface waves on an ideal fluid, *Stanford Univ. Tech. Rep. No.* 78, Math. & Stat. La. (1958).
6. R.J. Jarvis, The scattering of surface waves by two vertical plane barriers, *J. Inst. Maths. Applics.* 7 (1971) 207–215.
7. N.F. Parsons and P.A. Martin, Scattering of water waves by submerged curved plates and by surface-piercing flat plates. *Appl. Ocean Res.* 16 (1994) 129–139.
8. M. McIver and U. Urka, Wave scattering by circular arc shaped plates. *J. Engng. Maths.* 29 (1995) 575–589.
9. W.R. Dean, On the reflection of surface waves by a submerged circular cylinders, *Proc. Camb. Phil. Soc.* 44 (1948) 483–491.
10. F. Ursell, Surface waves on deep water in the presence of a submerged cylinder. Part I. *Proc. Camb. Phil. Soc.* 46 (1950) 141–152.
11. R.C. Thorne, Multipole expansions in the theory of surface waves. *Proc. Camb. Phil. Soc.* 49 (1953) 707–715.
12. P.A. Martin and R.A. Dalrymple, Scattering of long waves by cylindrical obstacles and gratings using matched asymptotic expansion. *J. Fluid Mech.* 108 (1988) 465–498.
13. P. McIver, Low frequency asymptotics of hydrodynamic forces on fixed and floating structures. In: M. Rahaman (ed.), *Ocean Wave Engineering*. Southampton: Computational Mechanics Publications U.K. (1994) pp. 1–49.